Performance Analysis of Small Cell and Distributed Antenna Systems for Indoor Mobile Communications

Temitope Alade* and Huiling Zhu†
* University of Worcester, †University of Kent, Canterbury, United Kingdom

***Abstract*—Fifth generation (5G) mobile communication systems aim to provide high data rate wireless transmissions and ubiquitous coverage to users but achieving this objective remains a challenge particularly in regions with high user density, such as urban/metropolitan areas and within buildings. To support users in indoor environments, indoor wireless communication systems are required, but frequency spectrum allocations are limited and requires reuse of the limited spectrum. Frequency reuse causes co-channel interference, which is detrimental to the performance and capacity of indoor systems. In order to design efficient and reliable indoor systems, a thorough understanding of co-channel interference within buildings is vital. This paper presents a comparative study of the performance of indoor deployed small cell base station (SBS) and indoor distributed antenna systems (DAS) in an isolated multi-storey building. Each floor of the building is equipped with either an indoor SBS or an indoor DAS where geographically distributed remote radio heads (RRHs) are connected to a central unit (CU), and frequency reuse is employed among floors. Signal propagation characteristics within multi-storey buildings and the impact of inter floor interference on system performance is analysed and compared for both systems. The effect of different reuse distances, pathloss exponents, penetration loss and co-channel interference on achievable rate is analysed over a wide range of potential mobile equipment (ME) locations.**

***Index Terms*—Distributed antenna system (DAS), Co-channel interference, Multi-floor in-building propagation, Spectral efficiency.**

I. Introduction

As the popularity of real-time data applications (apps) such as social networking apps and high-quality wireless video streaming increases, supporting a large number of users with high data rates remains a challenge for modern mobile communication systems, particularly in regions such as urban and metropolitan areas and within buildings. Providing adequate coverage and reliable system performance in these regions is difficult as, not only is the user density at its greatest, the communication traffic density and capacity demand can be extremely high. Furthermore, because the base station transmitters are generally located outside of buildings, large penetration losses are often encountered as the signal moves deeper into the interior of large buildings, thus limiting system performance and capacity [1].

To achieve adequate coverage and support increasing wireless traffic density within buildings, in-building wireless communication systems that will use small cells and employ extensive frequency reuse have been suggested. Among these are small cell base-stations (SBS) [2] [3] and distributed antenna systems (DAS) [4] designed to be located indoors to improve cellular system performance within small buildings, or across several floors of multi-storey buildings.

Indoor SBS are typically low-powered, short-range (10-50 m) cellular network base stations deployed within buildings, where each base station is a unique physical cell. Small cell densification using SBS is seen as an enabler for future 5G systems to address capacity demands [5]. However, to support a large number of users, multiple SBS are often required [6], necessitating the reuse of frequency spectrum. Frequency reuse introduces cochannel interference, which can severely limit system performance, reduce reliability, maximum transmission rates, and number of users that can be supported.

In indoor distributed antenna systems (DAS), remote radio heads (RRHs) are deployed to provide better coverage and improve system performance across several floors within a building. In contrast to indoor SBS where all service antennas are located in a compact area, the RRH are geographically distributed, effectively reducing the radio transmission distance between the transmitter and the receiver. The DAS thus reduces path loss, transmit power, and cochannel interference [7], thereby improving system performance, particularly for those mobile equipment (MEs) near the edge of a cell [8]. It is expected that the DAS will outperform SBS due to spatial diversity gain, however, it is not clear quantitatively how much of these gains can be achieved when compared with SBS for deployment in multi-storey buildings where frequency reuse is employed. Achieving adequate coverage for SBS or DAS is usually not an issue within buildings as the transmission distances are considerably shorter, rather it is co-channel interference that constrains performance.

The performance of cellular networks with co-located and distributed base-station antennas have been evaluated in many prior studies for outdoor environments where cell sizes are generally within thousands of meters. For example, [9], [10] and [11] compared the performance of co-located and distributed antennas and indicated that the distributed antenna layout has potential for higher data rates than co-located antenna layout. However, results obtained from these studies cannot be applied directly to in-building environments where a large number of potential users are distributed throughout a relatively small three-dimensional (3D) space, and divided

into smaller sub-spaces, such as in high-rise office buildings. Signal propagation in indoor systems occurs over shorter ranges than outdoor macro and microcellular systems and large losses can be experienced over very short distances. This is a major concern in multi-storey buildings where the same frequency channels may be reused on adjacent floors of the building to support a high density of users. Severe co-channel interference can occur and greatly limit the performance of the indoor system. Therefore, a thorough assessment of the way co-channel interference interacts with the 3D in-building environment is vital when planning indoor mobile communication systems.

This paper comparatively investigate the downlink performance of indoor deployed SBS and indoor DAS employing frequency reuse in a multi-storey building. Indoor radio channel propagation characteristics in multi-storey buildings, with frequency reuse among floors, and the resulting impact on system performance are examined and compared for both systems. Analysis of both line-of-sight (LOS) and non-LOS (NLOS) propagation conditions are considered.

II. Radio Propagation and Interference in Indoor Environments

Radio propagation in indoor environments differs from outdoor environments in a number of different ways [12]. For example, the distance between the transmitter and receiver, as well as propagation path lengths are typically much smaller (between 0-50 m); indoor environments are inherently 3D in topology and arguably more cluttered; both LOS and NLOS propagation paths exists, consequently, large losses can be experienced over a very short distance; signal losses are determined by floor plans, construction materials used, peoples' positions and movements, type and number of office equipment, scale of MEs used, and so on. Propagation studies presented in [13]-[15] for multi-storey buildings indicate that interference can arise via three propagation paths: 1) internal paths that involve transmission through the floor partitions, which may include multiple reflections between the walls, floors and ceilings; 2) external paths that involve transmission via diffraction down the window edges; 3) external paths that involve involve signal reflections and scattering from a nearby building. In an isolated multi-storey building (Fig. 1), the diffraction down the window edges is the only external path possible, however, its impact is insignificant and can be safely ignored [13].

III. Indoor Small-Cell System Model

Fig. 1(a) shows the downlink transmission of an indoor small-cell system in a multi-storey building where each floor of the building has one SBS centrally mounted on the ceiling to serve one ME on that floor. Each floor of the building has a similar construction with an open floor space plan, and frequency reuse is employed among the floors. There is no frequency reuse on the same floor, which implies that co-channel interference can only originate from adjacent floors. The worst case downlink performance of the indoor small-cell system is likely to occur when a ME is located in the corner of a floor, because at this location, the desired signal power will be weakest.

In the building, it is assumed there are a total of K SBS, one in each floor. Accordingly, K also denotes the number of floors in the building. The desired ME is located on the 4th floor of the building. Each floor has a common inter-floor spacing of F meters, and one active ME equipped with a single antenna is evenly located across each floor at height of v meters. The reuse distance C measured in floors, is the distance at which the frequency resource can be reused (Fig. 1 illustrates a reuse distance of three floors). Thus, FC is the total reuse distance in meters.

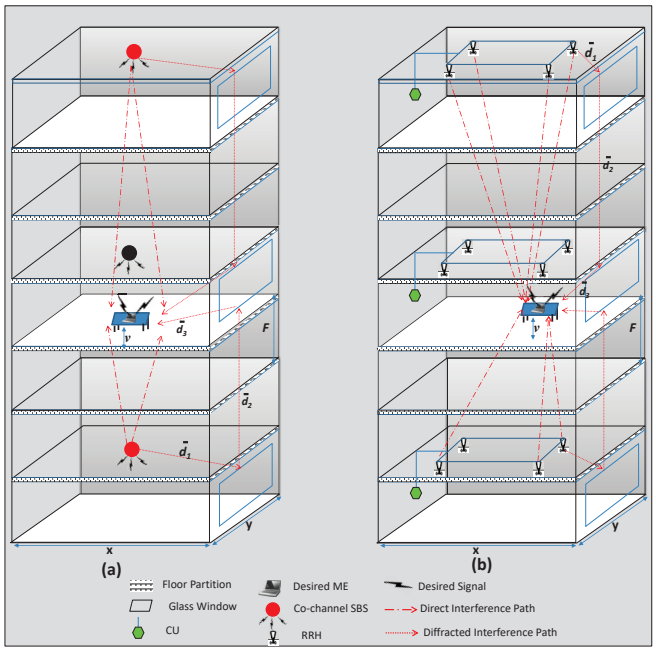

Fig. 1. (a) Indoor SBS with Frequency Reuse. (b) Indoor DAS with Frequency Reuse

The transmitted signal from SBS-k to the reference user is given by

$$X_k(t) = \sqrt{P_s} \sum_{i=-\infty}^{\infty} b_k[i]\, \rho_{T_s}(t - iT_s) \qquad (1)$$

where P_s denotes the transmit power which is assumed to be the same for all SBS, $b_k[i]$ is the transmitted symbol, T_s represent the symbol duration, $E[b_k] = 0$ and $E[b_k]^2 = 1$. $\rho_{T_s}(t)$ is a pulse waveform defined as $\rho_{T_s}(t) = 1$ for $0 \leq t \leq T_s$ and $\rho_{T_s}(t) = 0$ otherwise and f_c is the carrier frequency.

The channel between the SBS-k and reference user on the middle floor is given by the low pass equivalent impulse response as

$$h_k(t) = (d_k)^{-\mu/2} \cdot \tilde{\varphi}_k^{l/2} \cdot \alpha_k \cdot e^{j\theta_k} \cdot \delta(t - \tau_k) \qquad (2)$$

where d_k is the 3D path lengths from a SBS-k to the desired ME on the reference floor. Assuming a Cartesian coordinate system, where (x_k, y_k) represents the coordinate of the SBS-k, and (x, y) denotes the coordinate of the the desired ME on the reference floor, d_k can be written as

$$d_k = \sqrt{(x_k - x)^2 + (y_k - y)^2 + [Fl + (v - F)]^2} \qquad (3)$$

In (2), μ is the path loss exponent, typically varies between 2 to 6 depending on the physical layout and construction of the building [16]. $\tilde{\varphi}_k$ is the penetration loss through a single floor and l is the number of floors in the transmission path. α_k, θ_k and τ_k are the channel fading factor, path phase, and path delay, respectively, and are statistically independent. It is assumed that θ_k and τ_k are uniformly distributed over $[0, 2\pi]$ and $[0, T_s]$, respectively. $\delta(t)$ denotes the Dirac delta function.

Accordingly, the received lowpass equivalent signal at the reference user is given by

$$\begin{aligned} y(t) &= \sum_{k=1}^{K} X_k(t) \otimes h_k(t) + Z_0(t) \\ &= \sum_{k=1}^{K} (d_k)^{-\mu/2} \cdot \tilde{\varphi}_k^{l/2} \cdot \alpha_k \cdot e^{j\theta_k} \cdot X_k(t - \tau_k) + Z_0(t) \end{aligned} \tag{4}$$

where the notation $\otimes$ denotes the convolution operation and $Z_0(t)$ is the additive white Gaussian noise (AWGN) with zero mean and a double sided power spectral density $N_0/2$.

Assuming the phase and the path delay of the desired signal are precisely known at the receiver of the reference ME i.e, $\tau_{k'} = 0$, the demodulated signal over one symbol period T_s is given by

$$R = \frac{1}{T_s} \int_0^{T_s} y(t) \cdot e^{-j\theta_k} \; dt = S_0 + I_t + Z \tag{5}$$

where S_0 denotes the desired signal component received from the SBS on the reference floor, given by

$$\begin{aligned} S_0 &= \frac{1}{T_s} \int_0^{T_s} (d_{k'})^{-\mu/2} \cdot \alpha_{k'} \cdot e^{j\theta_{k'}} \cdot X_{k'}(t) \cdot e^{-j\theta_{k'}} dt \\ &= \sqrt{P_s} \cdot (d_{k'})^{-\mu/2} \cdot b_{k'} \cdot \alpha_{k'} \end{aligned} \tag{6}$$

I_t is the total co-channel interference term received by the reference user, given by

$$I_t = \sum\nolimits_{k=1, k\neq k'}^{K} I_k \tag{7}$$

where I_k is the co-channel interference component from other floors, given by

$$\begin{aligned} I_k &= \frac{1}{T_s} \int_0^{T_s} Q_r \cdot X_k(t - \tau_k) \cdot e^{-j\theta_{k'}} dt \\ &= \frac{Q_k}{T_s} \cdot \int_0^{T_s} X_k(t - \tau_k) dt \end{aligned} \tag{8}$$

where $Q_r = (d_k)^{-\mu/2} \cdot \tilde{\varphi}_k^{l/2} \cdot \alpha_k \cdot e^{j\theta_k}$, $Q_k = (d_k)^{-\mu/2} \cdot \tilde{\varphi}_k^{l/2} \cdot \alpha_k \cdot e^{j(\theta_k - \theta_{k'})}$. Since $E[\alpha_k^2] = 1$, $E[b_k] = 0$, $E[b_k \cdot b_k^*] = 1$ and $E[\tau_k^2] = E[(T_s - \tau_k)^2] = \frac{T_s^2}{3}$, the real and imaginary parts of I_k have the same variance derived as

$$\sigma_{I_k}^2 = \frac{P_s}{3} \cdot (d_k)^{-\mu} \cdot \tilde{\varphi}_k^l \tag{9}$$

The total co-channel interference term I_t is a zero mean Gaussian distributed random variable [17]. Thus, the expectation of I_k is a sum of complex Gaussian random variables easily derived as $E[I_t] = 0$ and the variance denoted by $\sigma_{I_t}^2$ is derived as

$$\begin{aligned} \sigma_{I_t}^2 &= E\left[I_t \cdot I_t^*\right] \\ &= \frac{P_s}{3} \sum\nolimits_{k=1, k\neq k'}^{K} (d_k)^{-\mu} \cdot \tilde{\varphi}_k^l \end{aligned} \tag{10}$$

Z in (5) is the noise component with zero mean and a variance of $\sigma_Z^2 = N_0/(4T_s)$, which is assumed to be equal for all SBS.

Thus, using (6) and (10), the instantaneous signal to interference plus noise ratio (SINR) γ at the reference ME is given by

$$\gamma = \frac{S_0^2}{\sigma_{I_t}^2 + \frac{N_0}{4T_s}} = \frac{P_s \cdot (d_{k'})^{-\mu} \cdot \alpha_{k'}^2}{\frac{P_s}{3} \sum_{k=1, k\neq k'}^{K} (d_k)^{-\mu} \cdot \tilde{\varphi}_k^l + \frac{N_0}{4T_s}} \tag{11}$$

According to various propagation studies, the possibility of a line of sight propagation is somewhat difficult to predict within buildings [18][19], particularly for SBS with colocated antennas. Consequently, it is assumed that the small scale fading $\alpha_{k'}$ is Rayleigh distributed. Thus, $\alpha_{k'}^2$ is exponentially distributed and the pdf of γ in (11) is given by

$$P_\gamma(\gamma) = \frac{1}{\bar{\gamma}} exp\left(-\frac{\gamma}{\bar{\gamma}}\right) \tag{12}$$

where $\bar{\gamma}$ is the average SINR for the reference ME given by

$$\bar{\gamma} = \frac{\frac{4E_s}{N_0}}{\frac{4}{3} \cdot \frac{E_s}{N_0} \sum_{k=1, k\neq k'}^{K} \left(\frac{d_k}{d_{k'}}\right)^{-\mu} + 1} \tag{13}$$

$\frac{E_s}{N_0}$ in (13) is the average received symbol energy-to-noise density ratio at the ME receiver location and E_s is expressed as

$$E_s = P_s \cdot T_s \cdot d_{k'}^{-\mu} \tag{14}$$

Therefore, the maximum possible rate of the indoor SBS system per floor for a giving location of the reference ME is given by

$$C_T = \int_0^\infty C_b \cdot log_2\left(1 + \gamma\right) P_\gamma(\gamma) d\gamma \tag{15}$$

where $C_b = 1/T_s$ is the channel bandwidth. The conditional rate per Hz is given by

$$C_c = \frac{C_T}{C_b} = \int_0^\infty log_2\left(1 + \gamma\right) P_\gamma(\gamma) d\gamma \tag{16}$$

By substituting (12) into (16), the conditional achievable rate per Hz C_c is rewritten as

$$\begin{aligned} C_c = &-log_2\left(1 + \gamma\right) \cdot exp\left(-\frac{\gamma}{\bar{\gamma}}\right)^\infty \\ &+ \int_0^\infty \frac{1}{(1 + \gamma) \cdot ln2} \cdot exp\left(-\frac{\gamma}{\bar{\gamma}}\right) d\gamma \end{aligned} \tag{17}$$

IV. INDOOR DAS MODEL

In this section, the system model and achievable rate expressions for indoor DAS is presented. These will be used in Section V to compare performance of indoor small cell system and indoor DAS.

For indoor DAS, the downlink transmission of the hypothetical building shown in Fig. 1(b) is considered, where each floor of the building is equipped with a CU comprised of $\bar{N}$ evenly spaced, ceiling mounted RRHs to serve MEs on each floor. Similar to the indoor small cell system, each floor is treated as a cell with the floors forming natural boundaries and frequency reuse is employed among the floors. In order to make a fair comparison between the indoor small cell systems and the indoor DAS, the same building geometry, same number of antennas per floor, same total transmit power per floor and same total system bandwidth are assumed for both systems.

In the downlink, the reference ME located in the middle floor of the building is served by one or more RRH in order to improve the received signal strength via spatial diversity [20]. Due to frequency reuse, the performance of the indoor DAS will depend on the strength of the desired signal and the relative strength of the interfering signals originating from nearby floors. Although the radio transmission distance between the transmitter and the receiver is further reduced in the indoor DAS due to geographically distributed RRH, the indoor DAS is exposed to strong cochannel interference, which can severely limit system performance as RRHs and MEs are located in close proximity.

In downlink transmission, since the signals transmitted from different RRHs experience different large scale fading, an efficient power allocation over the RRHs is necessary in order to significantly enhance the SINR at the ME and increase the achievable rate. Several power allocation strategies have been proposed in literature including the well known water filling solution, an optimal power allocation that maximizes the capacity when the channel state information is available at the transmitter. However, the water filling solution is very complicated, thus a simplified scheme proposed in [11] is employed to allocate tranmit power to the RRHs. Accordingly, the transmit power to be allocated to the nth RRH on the reference floor is given by

$$P_n = \frac{P_s \cdot \left(d_{n',k}\right)^{-\mu} \cdot \alpha^2_{n',k}}{\sum_{i=1}^{\bar{N}} \left(d_{n',i}\right)^{-\mu} \cdot \alpha^2_{n',i}} \tag{18}$$

where $d_{n',k}$ denotes the distance between the nth RRH and the ME on the reference floor. The distance $d_{n,k}$ is written as

$$d_{n,k} = \sqrt{(x_n - x)^2 + (y_n - y)^2 + [Ul + (v - U)]^2} \tag{19}$$

where (x_n, y_n) represents the coordinate of the nth RRH, and (x, y) denotes the coordinate of the the desired ME on the reference floor. Note that the number of intervening floors l between the desired ME and its target RRH on the reference floor is zero (i.e., l = 0). Assuming that the channel phase θ_n and the path delay $\tau_{n'}$ are precisely known at the nth RRH on the reference floor, the transmitted signal can be expressed as

$$X_{n,k}(t) = \sqrt{P_n} \cdot e^{-j\theta_{n,k}} . \sum_{i=-\infty}^{\infty} b_{n,k}\,[i]\,\rho_{T_s}(t - iT_s + \tau_{n',k}) \tag{20}$$

where $b_{n,k}$ denotes the transmitted symbol with $E[b_{n,k}] = 0$ and $E[b_{n,k}]^2 = 1$, and assumed to be the same for all RRHs.

The channel between the nth RRH and the reference ME on the middle floor is modelled as a low pass equivalent impulse response, given by

$$h_{n,k}(t) = (d_{n,k})^{-\mu/2} \cdot \tilde{\varphi}^{l/2}_{n,k} \cdot \alpha_{n,k} \cdot e^{j\theta_{n,k}} \cdot \delta(t - \tau_{n,k}) \tag{21}$$

where $\theta_{n,k}$ and $\tau_{n,k}$ are the path phase and path delay between the nth RRH and the reference user respectively, and are statistically independent. Given the geographical distribution of the RRHs, it is assumed that there is a possibility of LOS propagation between the nth RRH and the ME on the reference floor. Thus $\alpha_{n,k}$ undergoes Nakagami fading, hence, $\alpha^2_{n,k}$ is Gamma distributed with the probability distribution function (pdf) expressed as [21].

$$p_{\alpha^2_k}(\alpha^2_k) = \left(\frac{m_k}{\Omega_k}\right)^{m_k} \frac{(\alpha^2_k)^{m_k - 1}}{\Gamma(m_k)} \exp\left(-\frac{m_k}{\Omega_k}\alpha^2_k\right), \quad \alpha_{k'} \geq 0 \tag{22}$$

where m_k is the Nakagami factor and Ω_k is the average fading power of the received signal. The parameters Ω_k and m_k can be expressed as $\Omega_k = E[\alpha^2_k]$ and $m_k = \frac{\Omega^2_k}{E[(\alpha^2_k - \Omega_k)^2]}, m_k \geq \frac{1}{2}$ respectively. When $m_k = 1$, Nagakami fading reduces to Rayleigh fading [21].

Accordingly, the received lowpass equivalent signal at the reference ME is given by

$$\bar{y}(t) = \sum_{k=1}^{K} \sum_{i=1}^{\bar{N}} X_{n,k}(t) \otimes h_{n,k}(t) + \bar{Z}_0(t) \tag{23}$$

Assuming the receiver has a perfect timing synchronisation with the RRHs on the reference floor, i.e $\tau_{n',k} = 0$,, the demodulated signal over one symbol period T_s is given by

$$\bar{R} = \frac{1}{T_s} \int_0^{T_s} \bar{y}(t)dt = \bar{S}_0 + \bar{I}_t + \bar{Z} \tag{24}$$

where $\bar{S}_0$ denotes the desired signal component received from all RRHs located on the reference floor, given by

$$\begin{aligned} \bar{S}_0 &= \sqrt{\frac{P_s}{\sum_{i=1}^{\bar{N}} \left[d_{n',i}\right]^{-\mu} \cdot \alpha^2_{n',i}}} \cdot b_{n',k} \cdot \sum_{i=1}^{\bar{N}} \left[d_{n',k}\right]^{-\mu} \cdot \alpha^2_{n',k} \\ &= \sqrt{P_s} \cdot b_{n',k} \cdot \sqrt{\sum_{i=1}^{\bar{N}} \left[d_{n',k}\right]^{-\mu} \cdot \alpha^2_{n',k}} \end{aligned} \tag{25}$$

$\bar{I}_t$ is the total co-channel interference term received by the reference ME, given by

$$\bar{I}_t = \sum_{k=1, k \neq k'}^{K} \sum_{i=1}^{\bar{N}} \bar{I}_{n,k} \tag{26}$$

where $\bar{I}_{n,k}$ is the co-channel interference component from other floors, given by

$$\begin{aligned}\bar{I}_{n,k} &= \frac{1}{T_s}\int_0^{T_s} Q_d \cdot X_{n,k}(t-\tau_{n,k})dt \\ &= \frac{\bar{Q}_d}{T_s}\cdot\int_0^{T_s} X_{n,k}(t-\tau_{n,k})dt \end{aligned} \quad (27)$$

where $Q_d = (d_{n,k})^{-\mu/2}\cdot\tilde{\varphi}_{n,k}^{l/2}\cdot\alpha_{n,k}\cdot e^{j\theta_{n,k}}$, $\bar{Q}_d = (d_{n,k})^{-\mu/2}\cdot\tilde{\varphi}_{n,k}^{l/2}\cdot\alpha_{n,k}\cdot e^{j(\theta_{n,k}-\theta_{n',k})}$. Similar to the analysis in Section III, since $E[\alpha_{n,k}^2]=1$, $E[b_{n,k}]=0$, $E[b_{n,k}\cdot b_{n,k}^*]=1$ and $E[\tau_{n,k}^2]=E[(T_s-\tau_{n,k})^2]=\frac{T_s^2}{3}$, the real and imaginary parts of $\bar{I}_{n,k}$ have the same variance derived as

$$\sigma^2_{\bar{I}_{n,k}} = \frac{P_s}{3\cdot\bar{N}}\cdot(d_{n,k})^{-\mu}\cdot\tilde{\varphi}^l_{n,k} \quad (28)$$

The total co-channel interference term $\bar{I}_t$ is a zero mean Gaussian distributed random variable [17] and the variance denoted by $\sigma^2_{\bar{I}_t}$ is derived as

$$\begin{aligned}\sigma^2_{\bar{I}_t} &= E\left[\bar{I}_t\cdot\bar{I}_t^*\right] \\ &= \frac{P_s}{3\cdot\bar{N}}\sum_{k=1,k\neq k'}^{K}\sum_{i=1}^{\bar{N}}(d_{n,k})^{-\mu}\cdot\tilde{\varphi}^l_{n,k}\end{aligned} \quad (29)$$

$\bar{Z}$ in (24) is the noise component with a variance of $\sigma_Z^2 = N_0/(4T_s)$, which is assumed to be equal for all RRHs.

The instantaneous SINR $\bar{\bar{\gamma}}$ at the reference ME is given by

$$\bar{\bar{\gamma}} = \frac{\bar{S}_0{}^2}{\sigma^2_{\bar{I}_t}+\frac{N_0}{4T_s}} = \sum_{i=1}^{\bar{N}}\bar{\bar{\gamma}}_n \quad (30)$$

where $\bar{\bar{\gamma}}_n$ is given by

$$\bar{\bar{\gamma}}_n = \frac{\frac{4\bar{E}_s}{N_0}}{\frac{4}{3\bar{N}}\cdot\frac{\bar{E}_s}{N_0}\sum_{k=1,k\neq k'}^{K}\sum_{i=1}^{\bar{N}}\left(\frac{d_{n,k}}{d_{n',k}}\right)^{-\mu}\cdot\tilde{\varphi}^l_{n,k}+1}\cdot\alpha^2_{n',k} \quad (31)$$

$\frac{\bar{E}_s}{N_0}$ is the average received symbol energy-to-noise density ratio at the ME receiver location and $\bar{E}_s$ is expressed as

$$\bar{E}_s = P_s\cdot T_s\cdot d_{n',k}^{-\mu} \quad (32)$$

Assuming arbitrary values of the Nakagami fading parameters, the pdf of the instantaneous SINR, $\bar{\bar{\gamma}}_n$ in (31), is then obtained as [22]

$$P_{\bar{\bar{\gamma}}}(\bar{\bar{\gamma}}) = \frac{1}{\pi}\int_0^{\infty}\frac{\cos\left[\sum_{n=1}^{\bar{N}}m_n\tan^{-1}\left(\frac{t}{\beta_n}\right)-t\bar{\bar{\gamma}}\right]}{\prod_{n=1}^{\bar{N}}\left(1+\left(\frac{t}{\beta_n}\right)^2\right)^{m_n/2}}dt \quad (33)$$

where $\beta_n = m_n/\hat{\bar{\gamma}}_n$. $\hat{\bar{\gamma}}_n$ is the average SINR per RRH given by

$$\hat{\bar{\gamma}}_n = \frac{\frac{4\bar{E}_s}{N_0}}{\frac{4}{3}\cdot\frac{\bar{E}_s}{N_0}\sum_{k=1,k\neq k'}^{K}\sum_{i=1}^{\bar{N}}\left(\frac{d_{n,k}}{d_{n',k}}\right)^{-\mu}\cdot\tilde{\varphi}^l_{n,k}+1}\cdot\Omega_n \quad (34)$$

The maximum possible rate of the indoor DAS per floor for a giving location of the reference ME is given by

$$\bar{C}_T = \int_0^{\infty} C_b\cdot log_2\left(1+\bar{\gamma}\right)P_{\bar{\bar{\gamma}}}(\bar{\bar{\gamma}})d\bar{\gamma} \quad (35)$$

The conditional rate per Hz is derived by substituting (31) into (16), written as

$$\begin{aligned}\bar{C}_c = &\int_0^{\infty} log_2\left(1+\bar{\gamma}\right) \\ &\cdot\frac{1}{\pi}\int_0^{\infty}\frac{\cos\left[\sum_{n=1}^{\bar{N}}m_n\tan^{-1}\left(\frac{t}{\beta_n}\right)-t\bar{\bar{\gamma}}\right]}{\prod_{n=1}^{\bar{N}}\left(1+\left(\frac{t}{\beta_n}\right)^2\right)^{m_n/2}}dt\end{aligned} \quad (36)$$

V. Numerical Results

In this section, the achievable rate performance of the indoor SBS is compared with the indoor DAS using the analytic formulas derived in Sections III and IV for the hypothetical multi-storey building shown in Fig.1. For fair comparison, the same number of antennas per floor is assumed for both systems. MEs are assumed to be evenly located across the floor and 10000 possible ME locations are considered and used to numerically calculate the average value of the achievable rate across the entire floor. Unless otherwise stated, Table 1 presents the summary of parameters used in evaluating the performance of the systems.

Fig. 2 shows the average achievable rate of the indoor SBS and the indoor DAS for frequency reuse distances of $C = 1, 2$ floors. Note that a frequency reuse distance of 1 floor implies that the same frequencies are reused every floor, while in a reuse distance of 2 floors, channels are reused every second floor (co-channel interfering users are located on the 3rd, 5th and 7th floors). Clearly, superior performance is obtained with the indoor DAS over the indoor SBS. This is due to lower transmission path loss to the desired ME. In the indoor DAS, interfering signals experience a higher distance dependent rate of attenuation than that observed in the indoor SBS. Consequently, the received power by the desired ME dominates the performance and the resulting achievable rate is higher than that achieved with indoor SBS. It can be seen that increasing the reuse distance from one floor to two floors improves the performance of both systems significantly, especially at high SNR regions. This is due to high inter-floor isolation of co-channel floors which ensures high SINR, and high achievable rate across the floor. At high SNR values, the indoor DAS provides nearly 1 Bit/Sec/Hz increase in achievable rate over the indoor SBS for a reuse distance of 1 floor. Much larger achievable rates are observed for a reuse distance of two floors. At lower SNR values below 35dB, the achievable rate of both systems increase linearly and the the curves tend to be flat at SNR values more than about 40dB because co-channel interference dominates channel noise. Note that the performance of the indoor SBS tends to flatten more rapidly at higher SNR values because the system becomes more interference limited.

Fig. 3 shows the average achievable rate of the indoor SBS and the indoor DAS for a range of floor penetration losses with respect to frequency reuse distances of $C = 1, 2$ floors. A significant reduction in the total received signal to interference power is due to floor penetration losses. The penetration loss introduced by each floor depends on thickness of the floor inside the building and can vary from building to building. It is observed from the figure that the achievable rate of the indoor DAS are consistently higher than those of the indoor SBS. For both systems, the achievable rate increases as the penetration loss values increases. This is due to increase in the attenuation of the interfering signals. Results indicates that in buildings with low penetration loss less than 6dB, the indoor SBS may not tolerate a reuse distance of one floor due to low inter-floor isolation which results in low SINR, and low achievable rate values. Therefore an indoor DAS is mandatory in such buildings to ensure reliable wireless service.

Fig. 4 shows the average achievable rate of the indoor SBS and the indoor DAS for path loss exponent values $\lambda = 2, 3$. The internal layout of the building is known to play a significant role in determining the path loss exponent values. Lower path loss exponent values represent environments with fewer obstacles between the transmitter and the receiver, while higher values represents a NLOS environment with more obstructed paths. It is observed from Fig. 4 that the indoor DAS significantly outperforms the indoor SBS in both values of path loss exponent. For both systems, increasing the pathloss exponent value results in lower system performance. This is due to increase in the path loss of the desired signals. Although a higher path loss exponent value results in greater level of isolation from co-channel floors, thereby reducing the impact of co-channel interference. However, the power of the desired ME is also reduced due to increased path loss, resulting in lower spectral efficiency values. The indoor SBS are much more affected with by higher path loss exponent values. This is due to the fact that the indoor SBS antennas are co-located and thus experience approximately the same reduction in transmit signal power. This is not the case in indoor DAS as RRHs are geographically distributed. Note that at higher SNR values, channel noise dominated the performance and the achievable rate for $\lambda = 2, 3$ tends to merge for both systems.

VI. Conclusion

Indoor mobile communication systems are required to provide high data rate transmissions for mobile users located inside the building. However, these indoor system are likely to be deployed in dense in-building environments where the frequency channels are reused. This paper has comparatively analysed the performance of indoor SBS and indoor DAS employing frequency reuse. The in-building environment is mathematically defined and the performance of both systems is analytically quantified in terms of achievable rate for a 7-storey building. The propagation channel model is derived from multi-floor, in-building measurement data obtained from published propagation studies. It is been identified that superior performance is obtained with the indoor DAS over the indoor SBS. It is shown that in some buildings, it may be difficult to achieve adequate isolation between co-channel floors by increasing the reuse distance alone with an indoor SBS. For such buildings, an indoor DAS is therefore mandatory.

TABLE I
Summary of Parameters

Parameters	Value
Number of floors in the building, K	7
Inter-floor spacing, F	4m
Floor dimension, (x, y)	40m X 40m
ME located across the floor at height, v	1m
Reuse distance, C	1 floor
Number of RRH on each floor, N	4
Number of antenna on each floor	4
Path loss exponent, λ	2.5
Penetration loss, φ	13dB
Nakagami fading value, m	$1.8, 1.5, 1.25, 1.0$
Transmit SNR, E_s/N_0	30dB

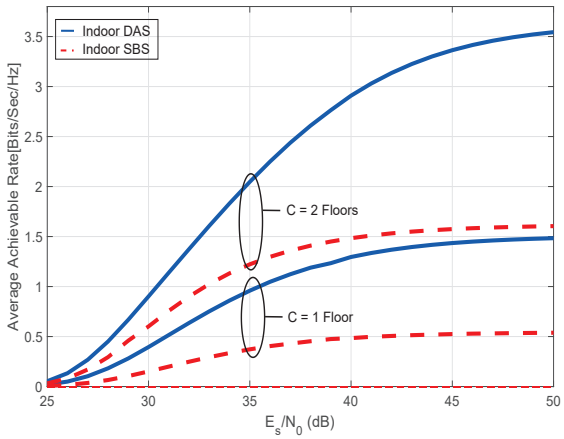

Fig. 2. Achievable rate comparison of indoor SBS and indoor DAS for different frequency reuse distances

References

[1] T. S. Rappaport, Y. Xing, G. R. MacCartney, A. F. Molisch, E. Mellios, and J. Zhang, "Overview of Millimeter Wave Communications for Fifth-Generation (5G) Wireless NetworksWith a Focus on Propagation Models", *IEEE Transactions on Antennas and Propagation*, vol. 65, pp. 62136230, December 2017.

[2] N. Bhushan et al., "Network densification: The dominant theme for wireless evolution into 5G"', *IEEE Commun. Mag.*, vol. 52, no. 2, pp. 82-89, Feb. 2014.

[3] M. Taranetz, R. W. Heath, and M. Rupp, "Analysis of Urban Two-Tier Heterogeneous Mobile Networks With Small Cell Partitioning", *IEEE Transactions on Wireless Communications*, vol. 15, no. 10, pp. 7044 - 7057, Oct. 2016.

[4] Y. D. Beyene, R. Jntti, K. Ruttik, "Cloud-RAN Architecture for Indoor DAS", *IEEE Access*, vol. 2, pp. 1205 - 1212, Oct. 2014.

[5] D. Lpez-Prez, M. Ding, H. Claussen, A. H. Jafari, "Towards 1 Gbps/UE in Cellular Systems: Understanding Ultra-Dense Small Cell Deployments", *IEEE Communications Surveys & Tutorials* , vol. 17, no. 4, pp. 2078 - 2101, June 2015.

[6] J. G. Andrews, H. Claussen, M. Dohler, S. Rangan, and M. C. Reed, "Femtocells: Past, present, and future", *IEEE Journal on Selected Areas in Communications*, vol. 30, no. 3, pp. 497 - 508, Apr. 2012.

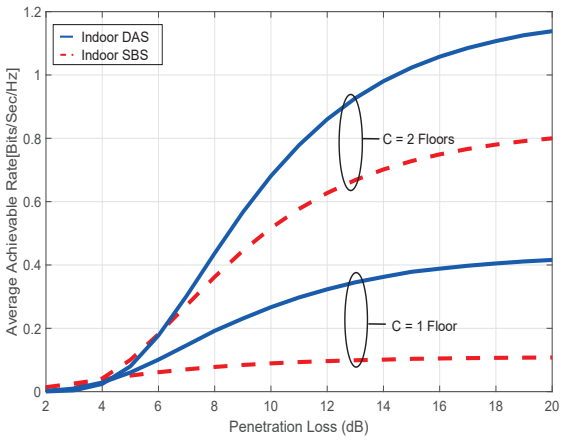

Fig. 3. Effect of penetration loss on achievable rate of indoor SBS versus indoor DAS for different reuse distances

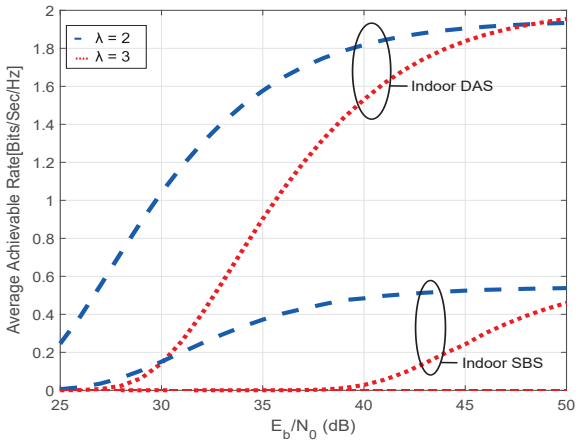

Fig. 4. Effect of path loss exponent on on achievable rate of indoor SBS versus indoor DAS

[7] W. Choi and J. G. Andrews, "Downlink performance and capacity of distributed antenna systems in a multicell environment", *IEEE Transactions on Wireless Communications*, vol. 6, no. 1, pp. 69 - 73, Jan. 2007.

[8] R. Heath, S. Peters, Y. Wang, and J. Zhang, "A current perspective on distributed antenna systems for the downlink of cellular systems", *IEEE Communication Magazine* vol. 51, no. 4, pp. 161 - 167, Apr. 2013.

[9] M. Clark, T. Willis III, L. Greenstein, A. Rustako Jr, V. Erceg, and R. Roman, "Distributed versus centralized antenna arrays in broadband wireless networks", *IEEE Vehicular Technology Conference, 2001*, VTC 2001 Spring. IEEE VTS 53rd, vol. 1. IEEE, 2001, pp. 33 - 37

[10] L. Dai, "A comparative study on uplink sum capacity with co-located and distributed antennas", *IEEE Journal on Selected Areas in Communications*, vol. 29, no. 6, pp. 1200 - 1213, June 2011.

[11] Huiling Zhu, "Performance Comparison between Distributed Antenna and Microcellular Systems," *IEEE Journal on Selected Areas in Communications*, vol. 29, no. 6, pp. 1151-1163, June 2011.

[12] Recom. ITU-R P.1238-6,"Propagation data and prediction methods for the planning of indoor radiocommunication systems and radio local area networks in the frequency range 900 MHz to 100 GHz"; 2017.

[13] M. A. Panjwani, A. L. Abbott, and T. S. Rappaport, "Interactive computation of coverage regions for wireless communication in multifloored indoor environments," *IEEE J. Select. Areas Commun.*, vol. 14, pp.420-430, Apr. 1996.

[14] W. Honcharenko, H. L. Bertoni and J. Dailing,"Mechanism governing propagation between different floors in buildings"; *IEEE Trans. Antennas Propagation*, vol. 41. no. 6, pp 787-790 June 1993.

[15] Andrew C. M. Austin, Michael J. Neve, Gerard B. Rowe and Ryan J. Pirkl, "Modelling the effects of nearby buildings on inter-floor radio wave propagation"; *IEEE Trans. Antennas Propagation*., vol. 57. no. 7, pp. 2155-2161 July 2009.

[16] K. Haneda et al., Indoor 5G 3GPP-like channel models for office and shopping mall environments, in 2016 IEEE International Conference on Communications Workshops (ICC), May 2016, pp. 694699.

[17] H. Yin, D. Gesbert, and L. Cottatellucci, "Dealing with interference in distributed large-scale MIMO systems: A statistical approach"; *IEEE J.Select. Topics Signal Process.*, vol. 8, no. 5, pp. 942-953, Oct. 2014.

[18] C. Oestges, N. Czink, B. Bandemer, P. Castiglione, F. Kaltenberger, and A. J. Paulraj, "Experimental Characterization and Modeling of Outdoor-to-Indoor and Indoor-to-Indoor Distributed Channels", *IEEE Transactions on Vehicular Technology*, vol. 59, pp. 22532265, June 2010.

[19] A. Ghosh et al., "Millimeter-wave enhanced local area systems: A high-datarate approach for future wireless networks"; *IEEE Journal on Selected Areas in Communications*, vol. 32, no. 6, pp. 1152-1163, June 2014.

[20] J. Park, E. Song, and W. Sungs, "Capacity analysis for distributed antenna systems using cooperative transmission schemes in fading channels"; emphIEEE Trans. Wireless Commun., vol. 8, no. 2, pp. 586-592, Feb. 2009

[21] L.-L. Yang and L. Hanzo, "Performance of generalized multicarrier DSCDMA over Nakagami-m fading channels," *IEEE Trans. Commun.*, vol. 50, no. 6, pp. 956-966, Jun. 2002.

[22] G. Efthymoglou and V. Aalo, "Performance of RAKE receivers in Nakagami fading channel with arbitrary fading parameters", *IEEE Electronic Letters*, Vol.31, No.18, pp. 1610-1612, Aug. 1995.